J. At. Mol. Sci.
doi: 10.4208/jams.021416.042116a

Vol. 7, No. 2, pp. 51-63
May 2016

Product angular and rovibrational state distributions of the Li + HF(v=0, j=0) → LiF(v′, j′) + H reaction

Xian-Fang Yue[a,b,*] and Ming-Chun Jiao[a]

[a] *Department of Physics and Information Engineering, Jining University, Qufu 273155, China*
[b] *Beijing Computational Science Research Center, Beijing 100193, China*

Received 14 February 2016; Accepted (in revised version) 21 April 2016
Published Online 25 May 2016

Abstract. A state-to-state dynamics analysis of the title reaction has been investigated via the quasiclassical trajecory method. Results of the product state resolved differential cross sections, polarization parameters, as well as rovibrational state distributions were revealed and discussed, most of which agree well with the recent quantum mechanics study by Roncero and co-workers. It was found that more than 82.28% of reactive trajectories undergo the direct reaction mechanism. The title reaction occurs predominantly in the head-end collision.

PACS: 33.15.Hp, 34.50.Lf, 79.20.Rf, 71.15.Pd

Key words: reaction mechanism, quasiclassical trajectory, differential cross section, polarization, product state distribution.

1 Introduction

As one of the simplest collision systems involving three different atoms, the Li + HF → LiF + H reaction has become a benchmark for the study of molecular reaction dynamics [1-35]. Experimentally, Becker *et al.* [1] have measured the laboratory angular distribution and time-of-flight spectra of LiF products in the reaction Li + HF → LiF + H at several collision energies by employing the crossed molecular beam (CMB) method. The analysis of their results in the center-of-mass (CM) frame demonstrates that the differential cross section (DCS) is nearly a forward-backward symmetry at the collision energy (E_c) of 130 meV, while a strongly forward peaked distribution at E_c=377 meV. Their observations on different DCSs were interpreted as a change in reaction mechanisms from the formation of a long lived complex at the low collision energy of 130 meV to a direct process at the

*Corresponding author. *Email addresses:* xfyuejnu@163.com (X.-F. Yue), jmch527@163.com (M.-C. Jiao)

high collision energy of 377 meV [1]. Loesch and co-workers [2-6] have performed a lot of CMB experiments on influences of reagent alignment [2], translational energy [3-4], vibrational [2, 5] and rotational excitations [6] on the Li + HF $\rightarrow$ LiF + H reaction. In their studies, the alignment of the reagent HF internuclear axis was achieved by changing the direction of the guiding field. The product angular distributions, the partition of available energy and integral reaction cross sections (ICSs) showed a marked difference for three different alignments of the HF internuclear axis (namely an isotropic distribution, two others with the molecular axis preferentially aligned along and perpendicular to the relative velocity vector of reagents). Recently, Bobbenkamp *et al.* [4] have implemented the effect of the excitation function (collision energy) on the ICS for the Li + HF $\rightarrow$ LiF + H reaction using a new CMB apparatus. A monotonous rise of the excitation function was found with the increase of energies ranging from 25 to 131 meV. This predicates that a possible translational energy threshold to the title reaction is significantly smaller than 25 meV, which supports the recent quantum mechanics (QM) study by Zanchet *et al.* [7] who have found a threshold of 10 meV.

Theoretically, a series of semi-empirical and *ab initio* potential energy surfaces (PESs) [8-14] have been constructed for the LiFH system. In 1980, Chen and Schaefer [8] have carried out the first *ab initio* PES calculation for this system by using the self-consistent field (SCF) and configuration interaction. The height of the barrier at the transition state (R_{LiF}=1.699Å, R_{HF}=1.291Å, θ_{LiFH}= 74°) was found to be 0.434 eV, which is too large for a realistic description of the reaction. Since then, a lot of *ab initio* calculations were dedicated to reduce the height of this reaction barrier. Carter and Murrell [9] reduced the barrier down to 0.17 eV. Laganà and co-workers [10] obtained the barrier of 0.182 eV at the bent transition state located in the exit channel. Aguado *et al.* [11-14] carried out multireference single and double excitation configuration interaction calculations of the LiFH PES. The number of 2323 *ab initio* points was computed and used to fit the PES. This PES shows a saddle point energy of 0.233 eV (from the minimum of the asymptotic entrance potential) located in the exit channel (R_{LiF}=1.692Å, R_{HF}=1.301Å, θ_{LiFH}= 71.4°). Availability of these reliable PESs has promoted numerous QCT [5-6, 15-20], time-independent quantum dynamics [21-26], and time-dependent wave packet [24-35] calculations to explore reaction dynamics of the Li + HF reaction. Most of these studies have verified that the title reaction contains rich and complex dynamics, and therefore further studies on reaction mechanisms are needed to carry out to elucidate dynamics of the Li + HF reaction.

At the present work, we carried out the state-to-state dynamics study on the Li + HF(v=0, j=0) $\rightarrow$ LiF(v', j') + H reaction at E_c = 97 meV by employing the QCT method. The product state resoled DCSs, first real polarization parameters, product rovibrational state distributions, and variations of internuclear distances and angles along the propagation time were calculated and presented. According to the direct interaction with product repulsion (DIPR) mode [36], we proposed a possible reaction mechanism which has rationally interpreted most of our calculated results.

2 Theoretical method

A latest *ab initio* PES for the ground state ($1^2A'$) of the LiFH system has been used in our calculations. This PES was developed by Aguado, Paniagua and Werner [14], therefore, it was also called APW PES in literatures. The energies and geometries of the reaction barrier and well in this PES are in reasonable agreement with previous ones in the Laganà *et al.* PES [10] and Aguado *et al.* PES [11-12]. The barrier height of the APW PES, 0.221 eV, is higher than that of the Laganà *et al.* PES (0.182 eV) [10], while slightly smaller than that of the Aguado *et al.* PES (0.233 eV) [12]. In the entrance channel, the complex well of the APW PES is -0.243 eV, which is shallower than that of the Aguado *et al.* PES (-0.279 eV) [12] or the Laganà *et al.* PES (-0.302 eV) [10]. Considering the zero-point energy effect, the exoergicity of the Li + HF(v=0, j=0) $\rightarrow$ LiF(v'=0, j'=0) + H reaction on the APW PES is ΔH_0^0 =-0.080 eV, which is slightly larger than that on the Laganà *et al.* PES (ΔH_0^0=-0.040 eV) [10], but somewhat smaller than that on the Aguado *et al.* PES (ΔH_0^0=-0.116 eV) [12]. Fig. 1 shows some features of the APW PES.

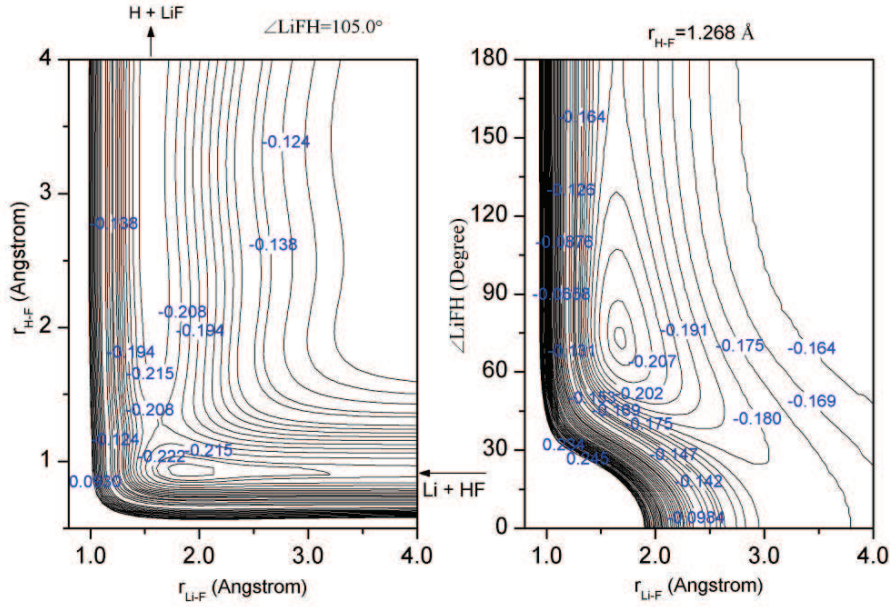

Figure 1: Two-dimensional cuts of the PES for configurations of the deep well in the entrance channel at ∠LiFH=105.0°(left panel) and the saddle point at r_{HF} = 1.268Å (right panel).

The QCT methodology used in the present study is the same as refs. 16-17 and 37-43. At the collision energy of 97 meV, batches of 1×10^5 trajectories have been calculated on the APW PES for the title reaction. With the sixth order gradient symplectic integrator method [43], an integration step of 0.1 fs ensured a conservation of total energy and total angular momentum better than 10^{-5} and 10^{-7}, respectively. Since the potential has

long range forces in both the entrance and exit channels, the trajectories are started and finished at a distance of 15.0Å between the Li atom and the CM of the HF molecule. The value of the maximum impact parameter, b_{max}, is 2.069Å. The value of b is selected by $b=\beta^{1/2}b_{max}$, where β is a random number in the [0, 1] interval. The orientation of the diatomic molecule, the phase of the diatomic vibrational motion, and β are randomly sampled by a Monte Carlo procedure. The vibrational and rotational levels of the reagent molecule are taken as v=0 and j=0, respectively. The atom mass is chosen to be 6.941 u for Li, 18.9984 u for F, and 1.008 u for H, respectively.

The CM frame was used as the reference frame in the present study, which is depicted in Fig. 2. The reagent relative velocity vector k is parallel to the z axis. The x-z plane is the scattering plane which contains the initial and final relative velocity vectors, k and k'. The θ_t is the angle between the reagent relative velocity and the product relative velocity (so-called scattering angle). The θ_r and ϕ_r are the polar and azimuthal angles of the final rotational angular momentum j'.

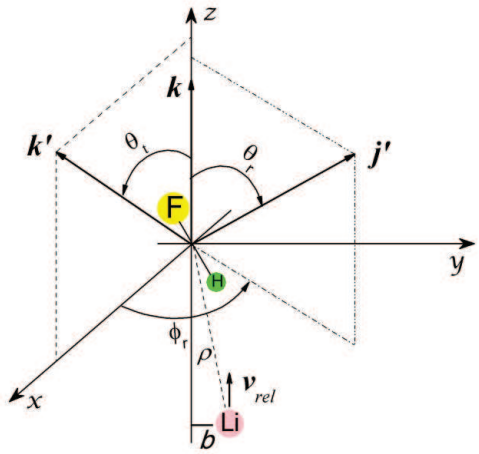

Figure 2: The center-of-mass coordinate system used to describe k, k' and j' correlations.

The differential cross section, $\frac{d\sigma_r}{d\omega}$, are calculated by the method of moments expansion in Legendre polynomials [44-46],

$$\frac{d\sigma_r}{d\omega}=\frac{\sigma_r}{2\pi}\left[\frac{1}{2}+\sum_{n=1}a_nP_n(\cos\theta_t)\right]. \tag{1}$$

Where the coefficients are given by

$$a_n=\frac{2n+1}{2}\langle P_n(\cos\theta_t)\rangle=\frac{2n+1}{2}\frac{1}{N_r}\sum_{i=1}^{N_r}P_n(\cos\theta_{ti}). \tag{2}$$

Here, $\sigma_r(=\pi b_{max}^2N_r/N_{tot}=0.62\text{Å})$ is the total integral reactive cross section. The angular

brackets represent the Monte Carlo average over the total number of reactive trajectories, N_r. N_{tot} is the total number of trajectories. A good convergence was achieved for the DCS when using the first seven Legendre moments in Eq. (1).

In order to describe the polarization degree of the product rotational angular momentum j', we have calculated the first real polarization parameters (PPs) $a_{1-}^{\{1\}}$ and $a_0^{\{2\}}$ [45-46]. Their expressions are

$$a_{1-}^{\{1\}} = \langle \sin\theta_j \sin\phi_j \rangle = \langle j'_y / j' \rangle, \tag{3}$$

$$a_0^{\{2\}} = \frac{1}{2}\langle 3\cos^2\theta_j - 1 \rangle = \frac{1}{2}\langle 3\frac{j'^2_z}{j'^2} - 1 \rangle. \tag{4}$$

Where j'_y and j'_z are the components of j' along the y and z axes, respectively. The $a_{1-}^{\{1\}}$ contains information on the orientation of the final rotational angular momentum j', while the $a_0^{\{2\}}$ reflects the alignment of the j'.

3 Results and discussion

Fig. 3 displays the total and vibrationally state resolved DCSs of the LiF products from the Li + HF(v=0, j=0) $\rightarrow$ LiF(v'=0-1, j') + H reactions. Clearly, DCSs for v'=0 (bottom panel in Fig. 3) and 1 (middle panel in Fig. 3) are preferentially forward scattered, so the total DCS (top panel in Fig. 3) favors forward scattering. The behavior of these DCSs distributions reveals a direct reaction mechanism for the title reaction. Note that the DCS of the LiF products for v' = 0 is very larger than that for v' = 1, meaning that most of the LiF products are in the ground vibrational state. The product rovibrational state distributions will be discussed later. In 2009, Roncero's group [7] carried out the first exact QM calculations on the DCSs of the title reaction at E_c = 97, 110, 136, 213 and 241 meV by employing a new wave packet code of MAD-WAVE3. At E_c = 241 meV, they computed the vibrationally state resolved DCSs of the Li + HF(v=0, j=0) $\rightarrow$ LiF(v'=0-2, j') + H reactions. It was found that the DCS favors forward scattering for v'=0, backward scattering for v'=1, and sideways scattering for v'=2. Very recently, his group [35] investigated the role of reactants polarization on the DCS for the state-to-state Li + HF(v, j, m) $\rightarrow$ LiF(v', j', Ω') + H reactions. At the collision energies of E_c = 110, 203 and 317 meV, vibrationally state resolved DCSs of the LiF products from the Li + HF(v=0, j=1-3) $\rightarrow$ LiF(v'=0-2, j') + H reactions were calculated. They found that the LiF(v'=0) products were preferentially forward scattered, while the vibrationally excited LiF(v'=1 and 2) were backward scattered. The behavior of our calculated DCS for the LiF(v'=0) agrees well with that of Roncero's study [7, 35]. Nevertheless, the DCS for the LiF(v'=1) shows contrary behavior between our QCT results (forward scattering) and Roncero's QM ones (backward scattering). For the total DCSs showed in the top panel of Fig. 3, our results demonstrate a good agreement with previous QCT calculations by Bobbenkamp *et al.* [6], however, it is inconsistent with recent QM results by Roncero's group [7, 35]. The QM total DCS [7,

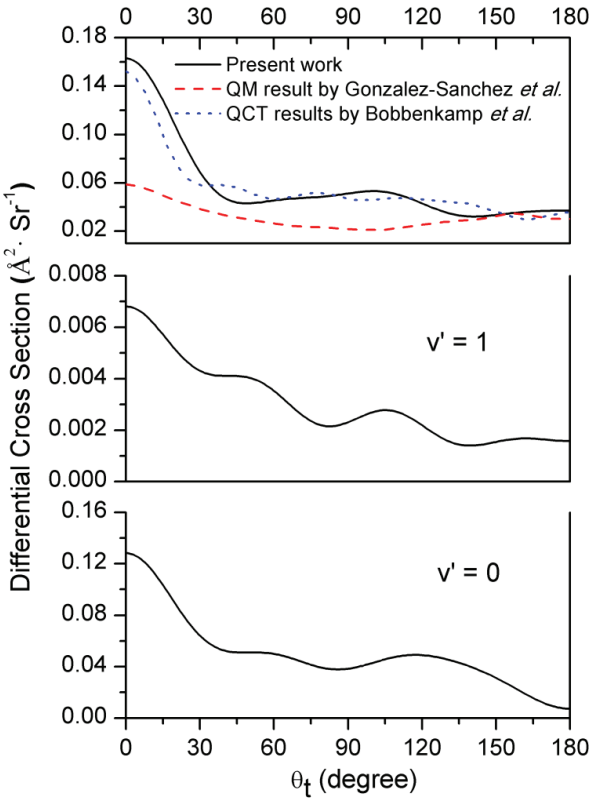

Figure 3: Vibrationally resolved DCSs of the LiF products from the Li + HF(v=0, j=0) → LiF(v', j') + H reaction for v'=0 (bottom panel) and 1 (middle panel). The top panel shows the total DCS compared with previous QCT DCS from Ref. 6 and QM DCS from Ref. 7.

35] presents both forward and backward scattering, however, only the forward scattering does it shows for the QCT total DCS. These differences were attributed to quantum effects, such as the transition state resonances [7, 35].

In order to penetrate into reaction mechanism of the title reaction, we have observed evolutionary trajectories of numerous reactive collision processes over the propagation time. Fig. 4 plots variations of three internuclear distances of the Li-F, F-H and H-Li, as well as three internuclear bond angles of the ∂LiFH, ∂FHLi and ∂HLiF as a function of propagation time. In the light of collision time, the reactive trajectories can be divided into two types. One (type I) undergoes a short collision time ($\leq$ 2.0 ps), as like as the process demonstrated in the left panels of Fig. 4. As an example of type I, the top left panel of Fig. 4 displays the evolution of three internuclear distances for one typical reactive trajectory, which manifests that the Li atom collides with the HF molecule and forms the LiF product that moves away immediately. Therefore, the reactive collisions corresponding to type I experienced the direct reaction mechanism. Fig. 5 shows percentage

of reactive trajectories as a function of collision time. According to the statistical analysis, at least 82.28 percent of the total reactive trajectories are type I. The other (type II) suffers a slightly longer collision time ($\geq$ 2.0 ps), as like as the process presented in the right panels of Fig. 4. As an instance of type II, the top right panel in Fig. 4 depicts the evolution of three internuclear distances for one representative reactive trajectory, which indicates that the Li atom collides with the HF molecule and forms a short-lived complex LiFH ($\approx$ 1.1 ps), then dissociates into the LiF products right away (top right panel in Fig. 4). As a consequence, the reactive collisions for type II experienced the indirect reaction mechanism. It can be seen from Fig. 5 that less than 17.72 percent of the total reactive trajectories are type II. To sum up, the title reaction has a dominant direct reaction mechanism and a minor indirect reaction mechanism.

As shown in the bottom panels of Fig. 4, the attacking angle of ∂FHLi is initially about 150° for the direct reactive collision (bottom left panel in Fig. 4), while it is about 120° for the indirect reactive collision (bottom right panel in Fig. 4). It was found that, for

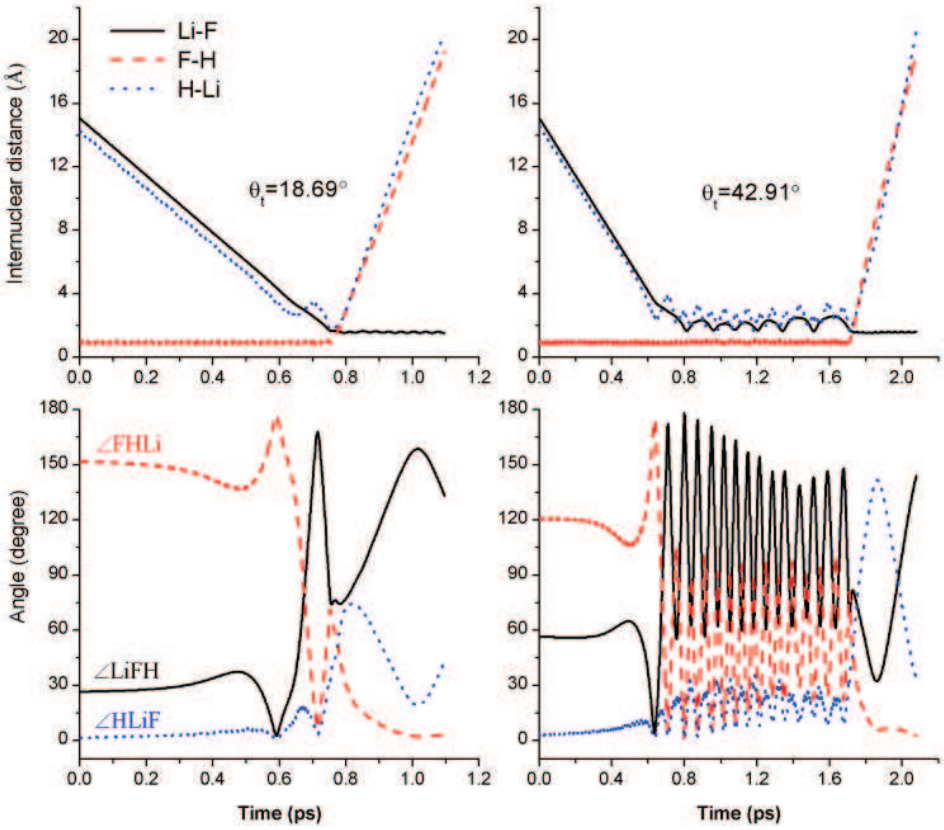

Figure 4: Variations of three internuclear distances (top panels) and bond angles (bottom panels) with propagation time.

most of the reactive trajectories, the initial attacking angles of ∂FHLi ranging from ∼110° to ∼170°, while the ∂HLiF is close to 0°. With the collision time propagating, a nearly collinear configuration of LIL H-F is formed displayed in both the bottom left (0.59 ps) and right panels (0.63 ps) of Fig. 4. That is to say, when the Li atom attacks the HF molecule from the H-end with a large angle of ∂FHLi, the title reaction is easiest to occur. This observation is coincident with previous QM [7, 35] and QCT [6] results. According to "Polanyi rules", the vibrational energy is more efficient than the translational energy in activating a late barrier reaction, whereas the reverse is true for an early barrier. The Li + HF reaction has a late barrier. The head-end attack from the Li atom to the H-end of the HF molecule favors the target molecule vibration, thus the reaction becomes advantageous. Therefore, the preference for reactions with the head-end collisions is ascribed to the late barrier.

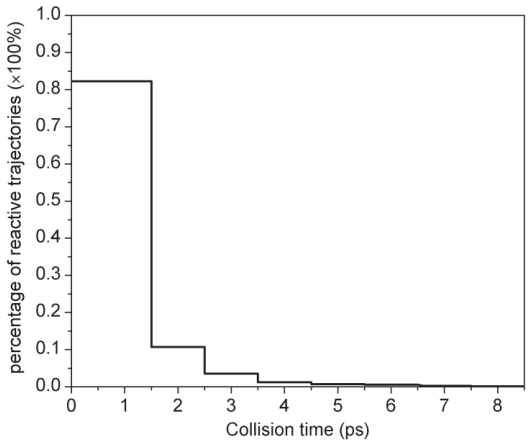

Figure 5: Percentage of reactive trajectories as a function of collision time.

The reaction mechanism can also be reflected by the opacity function of P(b) that is depicted in Fig. 6. Apparently, the title reaction is more favorable in small impact parameter collisions, which is the feature of the direct reaction mechanism. Fig. 7 shows the product state distributions and rotationally state resolved first polarization parameters for the Li + HF(v=0, j=0) → LiF(v'=0-1, j') + H reaction. As shown in Fig. 7(a), most of the LiF products from the title reaction are in the ground vibrational state v'=0 (≈ 94.39%), and the remaining are in the first vibrationally excited state v'=1. The rotational state distributions are inverted for both the v' = 0 and 1 states, and highly excited up to j' = 30 for v' = 0 and j' = 24 for v' = 1. Fig. 7b shows values of the $a_{1-}^{\{1\}}$ as a function of the rotational quantum number j'. Obviously, all the values of the $a_{1-}^{\{1\}}$, except for the product with v'=1, j'=1 and 2, are negative. As definition in Eq. (3), $a_{1-}^{\{1\}}$ (=$\langle \sin\theta_j \sin\phi_j \rangle$) contains information on the orientation of j' along the y-axis. Its minimum value is -1 and corre-

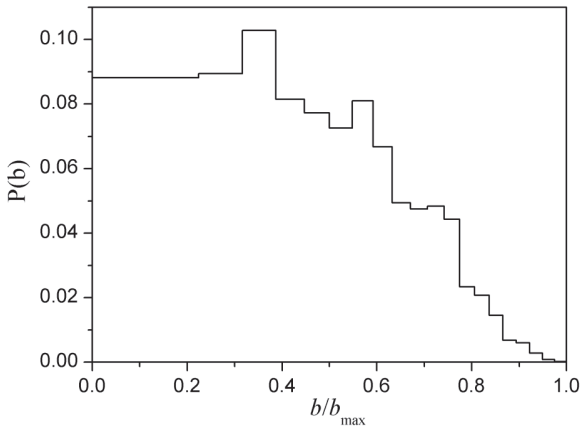

Figure 6: Reactive probability as a function of the impact parameter (opacity function).

sponds to the situation that j′ orientate along the negative y-axis. Correspondingly, the maximum value is +1, indicating that j′ preferentially orientate along the positive y-axis. Because the range of q_j is 0, q_j = 180, sinθ_j greater than or equal to 0. At present, the values of the $a_{1-}^{\{1\}}$ are negative, and so sinϕ_j must be negative. That is to say, the range of f_j is 180 f_j 360, implying that the orientation of the product rotational angular momentum j′ points to the hemisphere along the negative y-axis. Once the rotational quantum number j′ $\geq$ 5, the values of the $a_{1-}^{\{1\}}$ are close to -1, meaning that the orientation of j' aligns primarily along the negative y-axis. The statistical average value of $a_{1-}^{\{1\}}$ is -0.76 over all the products, suggesting that the orientation of the product rotational angular momentum j' is preferentially along the negative y-axis. Fig. 7c displays the values of the alignment parameter for the LiF products. As expressed in Eq. (4), the value of the $a_0^{\{2\}}$ equal to -1 when q_j = 90°, and at this moment the alignment of j' is exactly perpendicular to the k. For the Li + HF(v=0, j=0) $\rightarrow$ LiF(v′, j′) + H reaction, all the values of the $a_0^{\{2\}}$ are negative, and they approach to -1 for the products with the large rotation quantum number j'. The statistical average value of the $a_0^{\{2\}}$ for all the products is -0.84, which means that alignment of the product rotational angular momentum j' is preferentially along the direction perpendicular to the k. Our results are in excellent agreement with recent QM results by González-Sánchez *et al.* [35]. In their study, the calculated alignment was close to -1. That is the product rotational angular momentum is not only preferentially aligned perpendicular to the k, but also underlying oriented to the negative y-axis.

For reactions involving alkali metal atoms, the reaction mechanism has been regularly interpreted by the direct interaction with product repulsion (DIPR) mode proposed originally by Kuntz and co-workers [47-49]. As a representative reaction between alkali metal atom and hydrogen halide molecules, the reactive collision process could be rationally explicated by the DIPR mode. Combining the evolution of the reactive trajectory showed

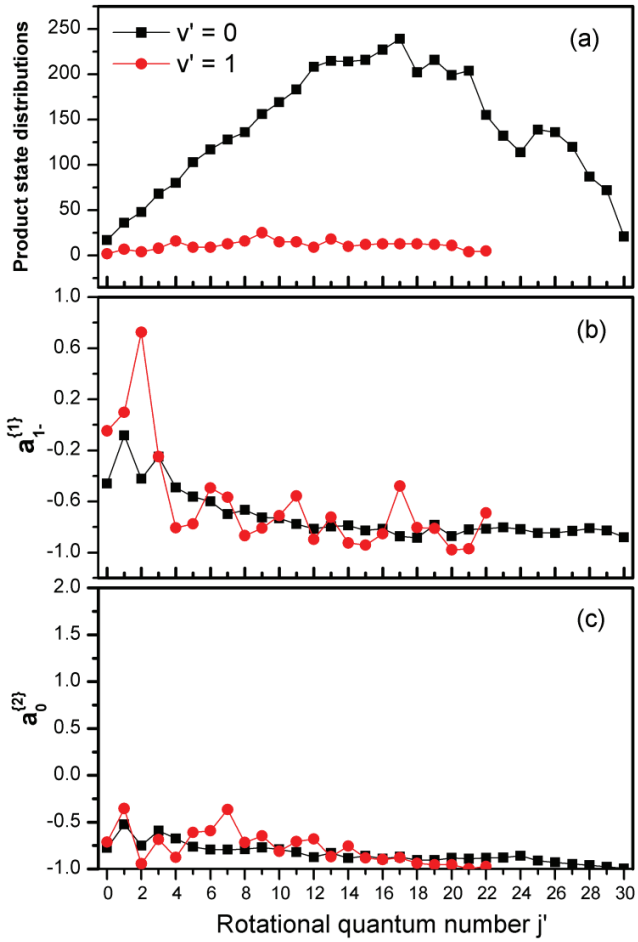

Figure 7: Product rotational state distributions (top panel) and values of the first real polarization parameters of $a_{1-}^{\{1\}}$ (middle panel) and $a_{0}^{\{2\}}$ (bottom panel) as a function of rotational quantum number j'.

in the left panels of Fig. 4 and the DIPR mode, we present a cartoon to describe the reaction mechanism for the title reaction in Fig. 8. Initially, the Li atom approaches the H-end of the HF molecule with a large angle of ∂FHLi and a long distance between the Li atom and the CM of the HF molecule (displayed in Fig. 8(a)). As the Li atom approaching, the Li atom would impel the H atom to close the F atom, and therefore the HF molecule is evoked to vibrate. The vibration of the reagent HF significantly facilitates the reaction to occur in the light of "Polanyi rules" that the reagent vibration would highly enhance the reaction probability for the reaction system with late barrier reaction. This can explain why the title reaction favors the head-end collision reaction. Under the mutual interaction of the relative reagent velocity and van der Waals forces, the Li atom will arrives at

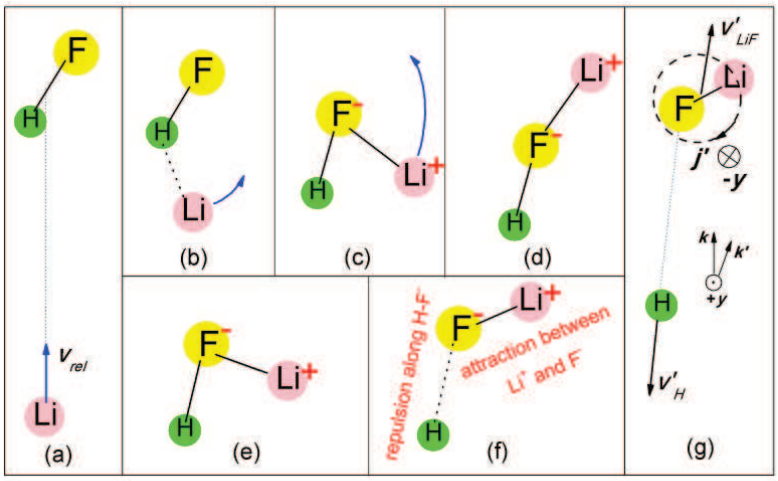

Figure 8: Cartoon illustration of the direct reaction mechanism in the light of the DIPR model (Ref. 36).

the F-end of the HF molecule (displayed in Fig. 8(d)) via intermediate configurations as like as showed in Figs. 8(b) and 8(c). Meanwhile, an electron of the Li atom "jump" to the F atom, and hence the ionic electronic state of the HLi^+F^- system is formed. Coulomp force between the Li^+ and the F^- shortens rapidly the internuclear distance of the LiF. On the ionic electronic PES, the Li atom comes back to the bent geometry of the saddle point depicted in Fig. 8e. At the saddle point, the curve crossing occurs between the covalent and ionic electronic states, and then the LiFH system gets into its exit channel of LiF + H. Subunit of the HF^- has a strong repulsive potential curve (displayed in Fig. 8(f)), which impels the H atom depart quickly from the HLi^+F^- system and pushes the F^- to move. As described in Fig. 8(g), the repulsive energy of the HF^- leads to rotationally excited Li^+F^- products and forward scattering. During reactive encounter, the total angular momentum is conserved, i.e. $J = L+j = L''+j''$. Where J is the total angular momentum. L and L' are the reagent and product orbital momenta, respectively. j is the reagent rotational angular momentum, and here it is zero because the reagent rotational quantum number j of the HF molecule is zero. Accordingly, the conservation of angular momentum becomes $L = L'+j'$. Since L and L' are perpendicular to k and k', respectively, both of them are perpendicular to the scattering plane. Therefore, the product rotational angular momentum j' is perpendicular to the scattering plane, thus it is perpendicular to the k. This provides the reason why the average alignment value of j' is close to -1. Because the H atom is very light, its departing results in small angular momentum L'. The angular momentum conservation can be approximately expressed by $L \gg j'$. Consequently, not only the value but also direction of the product rotational angular momentum j' is close to the total angular momentum J. These inferences could interpret the results that the product rotational state is highly excited, and the orientation of the j' is along the negative y-axis.

4 Conclusion

In the present work, we carried out the QCT calculations on the Li + HF(v=0, j=0) $\rightarrow$ LiF(v′, j′) + H reaction under a latest PES and E_c = 97 meV. The vibrationally state resolved differential cross sections, product state distributions, evolution of three internuclear distances and bond angles over the propagation time, as well as the first real polarization parameters are calculated and analyzed. It was found that the vibrationally state resolved DCSs are preferentially forward scattered for both the vibrational states of v′=0 and 1, thereby, the total DCS favors the preferential forward scattering. Analysis of the product state distributions demonstrates that about 94.39% of the LiF products are in the ground vibrational state (v′=0), and the rest are in the first vibrationally excited state (v′=1). The rotational state distributions are inverted for both the vibrational states of v′ = 0 and 1, and highly excited up to j′ = 30 for the v′ = 0 state and j′ = 24 for the v′ = 1. The opacity function demonstrates that the smaller the impact parameter is, the higher the reaction probability is. Variations of three internuclear distances and bond angles reveal that only from the H-end of the HF molecule with a large angle of ∂FHLi does the Li atom attack the HF, the title reaction could occur. This observation is coincident with recent QM conclusion of Roncero's group. Analysis on evolution of reactive trajectories discloses that more than 82.28 percent of the total reactive events undergo the short collision time ($\leq$ 2.0 ps), that is to say, the reaction is dominantly the direct reaction mechanism. The average values of the first real polarization parameters $a_{1-}^{\{1\}}$ and $a_0^{\{2\}}$ are -0.76 and -0.84, respectively, which reveals that the product rotational angular momentum j' is not only aligned perpendicular to the k, but also oriented along the negative y-axis. These results are in good agreement with recent QM ones by Roncero's group. Employing the DIPR model, the author presented a cartoon to describe the reaction mechanism and nicely interpreted our calculated results.

Acknowledgments. The authors gratefully acknowledge the financial support provided by the National Natural Science Foundation of China (Grant No. 21003062 and 11447014), the Project of Shandong Province Higher Educational Science and Technology Program (Grant No. J14LJ09) and the China Postdoctoral Science Foundation (Grant No. 2014M550595).

References

[1] C. H. Becker, P. Casavecchia, *et al.* J. Chem. Phys. 73 (1980) 2833.
[2] H. J. Loesch and F. Stienkemeier, J. Chem. Phys. 98 (1993)9570.
[3] O. Höbel, R. Bobbenkamp, A. Paladini, *et al.* Phys. Chem. Chem. Phys. 6 (2004) 2198.
[4] R. Bobbenkamp, H. J. Loesch, M. Mudrich, *et al.*, J. Chem. Phys. 135 (2011) 204306.
[5] F. J. Aoiz, E. Verdasco, V. S. Rábanos, *et al.*, Phys. Chem. Chem. Phys. 2 (2000) 541.
[6] R. Bobbenkamp, A. Paladini, A. Russo, *et al.*, J. Chem. Phys. 122 (2005) 244304.
[7] A. Zanchet, O. Roncero, T. González-Lezana, *et al.*, J. Phys. Chem. A 113 (2009) 14488.
[8] M. M. L. Chen and H. F. Schaefer, J. Chem. Phys. 72 (1980) 4376.

[9] S. Carter and J. N. Murrell, Mol. Phys. 41 (1980) 567.
[10] G. A. Parker, A. Laganà, S. Crocchianti, *et al.* J. Chem. Phys. 102 (1995) 1238.
[11] A. Aguado, M. Paniagua, M. Lara, *et al.*, J. Chem. Phys. 106 (1997) 1013.
[12] A. Aguado, M. Paniagua, M. Lara, *et al.*, J. Chem. Phys. 107 (1997) 10085.
[13] A. W. Jasper, M. D. Hack, D. G. Trhular, *et al.*, J. Chem. Phys. 116 (2002) 8353.
[14] The FORTAN code of the PES is available in http://www.theochem.unistuttgart.de/potentials.html.
[15] F. J. Aoiz, M. T . Menéndez and V. S. Rábanos, J. Chem. Phys. 114 (2001) 8880.
[16] Y. Wang, K. Deng and R. Lu, J. At. Mol. Sci. 6 (2015) 11.
[17] X.-F. Yue and M.-S. Wang, Chem. Phys. 405 (2012) 155.
[18] J. M. Alvariño, P. Casavecchia, O. Gervasi, *et al.*, J. Chem. Phys. 77 (1982) 6341.
[19] A. W. Jasper, M. D. Hack, A. Chakraborty, *et al.*, J. Chem. Phys. 115 (2001) 7945.
[20] F. J. Aoiz, M. T. Marínez, M. Menéndez, *et al.*, Chem. Phys. Lett. 299 (1999) 25.
[21] G. A. Parker, A. Laganà, S. Crocchianti, *et al.*, J. Chem. Phys. 102 (1995) 1238.
[22] L. Wei, A.W. Jasper and D. G. Truhlar, J. Phys. Chem. A 107 (2003) 7236.
[23] A. Laganà, A. Bolloni and S. Crocchianti, *et al.*, Phys. Chem. Chem. Phys. 2 (2000) 535.
[24] M. Baer, I. Last and H. J. Loesch, J. Chem. Phys. 101 (1994) 9648.
[25] D. Skouteris, S. Crocchianti and A. Laganà, Chem. Phys. Lett. 440 (2007) 1.
[26] A. Laganà, A. Bolloni, S. Crocchianti, *et al.*, Chem. Phys. Lett. 324 (2000) 466.
[27] W. Zhu, D. Wang and J. Z. H. Zhang Theor. Chem. Acc. 96 (1997) 31.
[28] B. Zhou and Q. Wei, J. At. Mol. Sci. 6 (2015) 52.
[29] M. Paniagua, A. Aguado, M. Lara, *et al.*, J. Chem. Phys. 111 (1999) 6712.
[30] M. Lara, A. Aguado, O. Roncero, *et al.*, J. Chem. Phys. 109 (1998) 9391.
[31] M. Lara, A. Aguado, M. Paniagua, *et al.*, J. Chem. Phys. 113 (2000) 1781.
[32] A. Aguado, M. Lara, M. Paniagua, *et al.*, J. Chem. Phys. 114 (2001) 3440.
[33] S. Gómez-Carrasco and O. Roncero, J. Chem. Phys. 125 (2006) 054102.
[34] C. Sanz, O. Roncero, M. Paniagua, *et al.*, Chem. Phys. Lett. 351 (2002) 295.
[35] L. González-Sánchez, O. Vasyutinskii, A. Zanchet, *et al.*, Phys. Chem. Chem. Phys. 13 (2011) 13656.
[36] J.-M. Mestdagh, B. Soep, M.-A. Gaveau, *et al.*, Int. Rev. Phys. Chem. 22 (2003) 285.
[37] Z. X. Duan, W. L. Li and M. H. Qiu, J. Chem. Phys. 136 (2012) 144309.
[38] S. Liu and Y. Shi, Chem. Phys. Lett. 501 (2011) 197.
[39] J. Liu, M. Wang and A. Gao, J. At. Mol. Sci. 6 (2015) 129.
[40] K. L. Han, G. Z. He and N. Q. Lou, J. Chem. Phys. 105 (1996) 8699.
[41] M. L. Wang, K. L. Han and G. Z. He, J. Phys. Chem. A 102 (1998) 20204.
[42] K. L. Han, L. Zhang, D. L. Xu, *et al.*, J. Phys. Chem. A 105 (2001) 2956.
[43] X. Zhang and K.L. Han, Int. J. Quant. Chem. 106 (2006) 1815.
[44] D. G. Truhlar and N. C. Blais J. Chem. Phys. 67 (1977) 1532.
[45] F. J. Aoiz, M. Brouard and P. A. Enriquez, J. Chem. Phys. 105 (1996) 4964.
[46] F. J. Aoiz, M. T. Martínez and V. S. Rábanos, J. Chem. Phys. 114 (2001) 8880.
[47] P. J. Kuntz, E. Nemetz and J. C. Polanyi, J. Chem. Phys. 50 (1969) 4607.
[48] P. J. Kuntz, E. H. Mok and J. C. Polanyi, J. Chem. Phys. 50 (1969) 4623.
[49] P. J. Kuntz, Mol. Phys. 23 (1972) 1035.